PPARδ Activation Protects Endothelial Function in Diabetic Mice

Xiao Yu Tian,[1] Wing Tak Wong,[1,2] Nanping Wang,[3,4] Ye Lu,[1] Wai San Cheang,[1] Jian Liu,[1] Limei Liu,[1,5] Yahan Liu,[4] Susanna Sau-Tuen Lee,[6] Zhen Yu Chen,[6] John P. Cooke,[2] Xiaoqiang Yao,[1] and Yu Huang[1]

Recent evidence highlights the therapeutic potential of peroxisome proliferator–activated receptor-δ (PPARδ) agonists to increase insulin sensitivity in diabetes. However, the role of PPARδ in regulating vascular function is incompletely characterized. We investigate whether PPARδ activation improves endothelial function in diabetic and obese mice. *PPARδ* knockout (KO) and wild-type (WT) mice fed with high-fat diet and *db/db* mice were used as diabetic mouse models, compared with *PPARδ* KO and WT mice on normal diet and db/m^+ mice. Endothelium-dependent relaxation (EDR) was measured by wire myograph. Flow-mediated vasodilatation (FMD) was measured by pressure myograph. Nitric oxide (NO) production was examined in primary endothelial cells from mouse aortae. PPARδ agonist GW1516 restored EDRs in mouse aortae under high-glucose conditions or in *db/db* mouse aortae ex vivo. After oral treatment with GW1516, EDRs in aortae and FMDs in mesenteric resistance arteries were improved in obese mice in a PPARδ-specific manner. The effects of GW1516 on endothelial function were mediated through phosphatidylinositol 3-kinase (PI3K) and Akt with a subsequent increase of endothelial nitric oxide synthase (eNOS) activity and NO production. The current study demonstrates an endothelial-protective effect of PPARδ agonists in diabetic mice through PI3K/Akt/eNOS signaling, suggesting the therapeutic potential of PPARδ agonists for diabetic vasculopathy. ***Diabetes* 61:3285–3293, 2012**

Peroxisome proliferator–activated receptor-δ (PPARδ) is the least studied isoform of PPARs, and it is ubiquitously expressed in tissues such as liver, brain, skin, and adipose (1). Recently, the role of PPARδ in obesity and diabetes has been examined by using the loss-of-function approach or synthetic PPARδ ligands. Although it was reported that PPARδ deficiency may lead to reduced adipogenesis (2), the *PPARδ* knockout (KO) mouse is more prone to weight gain on a high-fat diet, whereas the *PPARδ* transgenic mouse is protected against obesity and lipid accumulation (3,4). PPARδ agonists GW501516/GW1516, GW0742, and L-165041 can improve the lipid profile in obese animal models through increasing levels of HDL and decreasing LDL cholesterol and triglycerides (5,6).

PPARδ also regulates glucose homeostasis and insulin signaling in various tissues (7–9). PPARδ activation in *db/db* mice improves hepatic and peripheral insulin sensitivity by increasing glucose consumption in the liver (10). GW0742 treatment or hepatic overexpression of PPARδ attenuates fatty liver and nephropathy in diabetic mice (11,12). In human subjects, GW1516 enhances the HDL level and facilitates triglyceride clearance in healthy individuals by upregulation of fatty acid oxidation in skeletal muscle (13). GW1516 can also lower plasma levels of triglyceride, LDL cholesterol, and insulin in obese men (14). In general, PPARδ is beneficial against obesity, insulin resistance, and metabolic syndrome.

The metabolic functions of PPARδ are likely to be associated with cardiovascular benefits in diabetes. PPARδ is an important transcriptional factor in myocardial metabolism (15,16). PPARδ activation inhibits oxidative stress and inflammation and prevents myocardial hypertrophy in diabetic mice (17). However, the direct effects of PPARδ activation on vascular processes such as angiogenesis and endothelial function are less studied. PPARδ is expressed in endothelial cells (18). Importantly, prostacyclin, which can be released by the endothelium, promotes proangiogenic function in a PPARδ-dependent manner (19). PPARδ agonists enhance the regenerative capacity of endothelial progenitor cells (20,21) and protect endothelial cells from apoptosis (22). PPARδ agonist also inhibits vascular inflammation and reduces atherosclerotic lesions in mouse models (23–26). These experimental observations suggest that PPARδ may play a positive role in vascular activities such as angiogenesis, apoptosis, vascular inflammation, and endothelial vasodilatory function.

Notably, the effect of the PPARδ activator GW1516 to enhance vasculogenesis is reported to be mediated by the phosphatidylinositol 3-kinase/Akt (PI3K/Akt) signaling pathway (20,21). GW0742 can induce vasodilatation through PI3K/Akt and reduce blood pressure in hypertensive rat (27,28). Up to date, no study has examined the possible role of PPARδ in endothelial dysfunction related to diabetes and obesity. Therefore, the current study investigated the effect of PPARδ activation on endothelial dysfunction in diabetic mice and determined whether or not PI3K/Akt could contribute to the vascular benefit of PPARδ activation.

RESEARCH DESIGN AND METHODS

Animal protocols. Male C57BL/6 mice, leptin receptor KO (*db/db*), with their lean db/m^+ littermates (both at the age of 12–14 weeks) (*PPARδ* KO mice and *PPARδ* WT [wild type]) generated from C57BL/6N × Sv/129 background were used for this study. *PPARδ* WT and *PPARδ* KO mice were generated as described previously (1). This mouse line has been verified by several studies

From the [1]Institute of Vascular Medicine, Li Ka Shing Institute of Health Sciences, School of Biomedical Sciences, The Chinese University of Hong Kong, Hong Kong, China; the [2]Division of Cardiovascular Medicine, Department of Medicine, Stanford University School of Medicine, Stanford, California; the [3]Cardiovascular Research Center, Xi'an Jiaotong University, Xi'an, China; the [4]Institute of Cardiovascular Science, Peking University Health Science Center, Beijing, China; the [5]Department of Physiology and Pathophysiology, Peking University Health Science Center, Beijing, China; and the [6]School of Life Sciences, The Chinese University of Hong Kong, Hong Kong, China.

Corresponding author: Yu Huang, yu-huang@cuhk.edu.hk, or Nanping Wang, npwang2010@mail.xjtu.edu.cn.

Received 2 February 2012 and accepted 15 June 2012.

DOI: 10.2337/db12-0117

This article contains Supplementary Data online at http://diabetes.diabetesjournals.org/lookup/suppl/doi:10.2337/db12-0117/-/DC1.

X.Y.T. and W.T.W. contributed equally to the work.

(1,10,29). The mice were housed in a temperature-controlled holding room (22–23°C) with a 12-h light/dark cycle and fed standard chow and water. All of the experiments were approved by the institutional animal care and use committee and were consistent with the Guide for the Care and Use of Laboratory Animals published by the National Institutes of Health. Diet-induced obese (DIO) mice were generated on *PPARδ* KO, age-matched *PPARδ* WT littermates, and C57BL/6 mice at the 6 weeks of age and were fed for 10–12 weeks with a high-fat diet (rodent diet with 45% kcal [% fat], D12451; Research Diets, Inc., New Brunswick, NJ). Mice were treated with GW1516 or vehicle (0.5% cellulose) by oral gavage at the dosage of 5 mg/kg/day for 7 days, 12 weeks after high-fat feeding.

Functional assay by wire myograph. After mice were killed, thoracic aortae were removed and placed in oxygenated ice-cold Krebs solution that contained (mmol/L) 119 NaCl, 4.7 KCl, 2.5 $CaCl_2$, 1 $MgCl_2$, 25 $NaHCO_3$, 1.2 KH_2PO_4, and 11 D-glucose. Changes in isometric tone of the aortic rings were recorded in myograph (Danish Myo Technology, Aarhus, Denmark). The rings were stretched to an optimal baseline tension of 3 mN and then allowed to equilibrate for 60 min before the experiment commenced. Rings were first contracted with 60 mmol/L KCl and rinsed in Krebs solution. After several washouts, phenylephrine (1 μmol/L) was used to produce a steady contraction, and acetylcholine (ACh) (10 nmol/L to 10 μmol/L) was added cumulatively to induce endothelium-dependent relaxation (EDR). Endothelium-independent relaxation to sodium nitroprusside (SNP) was performed in aortic rings, with endothelium removed by gently rubbing with fine forceps.

Ex vivo culture of mouse aortic rings. Mouse thoracic aortic rings (2 mm in length) were dissected in sterile PBS and incubated in Dulbecco's modified Eagle's medium (DMEM; Gibco, Gaithersburg, MD) supplemented with 10% FBS (Gibco), plus 100 IU/mL penicillin and 100 μg/mL streptomycin. Drugs, including GW1516 (PPARδ agonist, 0.1 μmol/L; Alexis Biochemicals, Lausen, Switzerland), GW0742 (PPARδ agonist, 0.1 μmol/L; Tocris Bioscience, Bristol, U.K.), GSK0660 (PPARδ antagonist, 1 μmol/L; Sigma-Aldrich, St. Louis, MO), LY294002 (PI3K inhibitor, 5 μmol/L; Tocris), wortmannin (PI3K inhibitor, 0.1 μmol/L; Sigma-Aldrich), and Akt inhibitor V (API-2/triciribine, 5 μmol/L; Sigma-Aldrich) were individually added into the culture medium that bathed the aortic rings. High-glucose (HG) conditions were achieved by the addition of 25 mmol/L glucose, whereas 25 mmol/L of mannitol was used as the normal glucose (NG) osmotic control. After the incubation period, the rings were transferred to a chamber filled with fresh Krebs solution and mounted in a myograph for measurement of changes in isometric force. Acetylcholine, phenylephrine, and SNP were dissolved in water and others in DMSO.

Functional assay by pressure myograph. Mesenteric resistance arteries were dissected and cannulated between two glass cannulas as previously described (30). The vessel diameter was monitored by a Zeiss Axiovert 40 microscope, model 110P, with video camera monitored with the Myo-View software (Danish Myo Technology, Aarhus, Denmark). Contraction was induced by 10 μmol/L phenylephrine after the vessel stabilized at 100 mmHg intraluminal pressure, and flow-mediated vasodilatation (FMD) was induced by pressure change, which equals ~15 dynes/cm^2 shear stress. After washout, insulin-induced vasodilatation was examined in phenylephrine-contracted arteries. Passive dilation was tested at the end of experiment in the Ca^{2+}-free Krebs solution with 2 mmol/L EGTA. FMD data were expressed as percent of diameter changes = (flow-induced dilation − Phe tone)/(passive dilation − Phe tone).

Ex vivo adenoviral gene transfer in mouse aorta. The infection protocol in mouse aortic rings ex vivo was described previously (31). Adenovirus encoding constitutively activated PI3K (Ad-CA-PI3K) and constitutively activated Akt (Ad-CA-Akt) were described previously (32). Adenovirus encoding dominant-negative Akt (Ad-DN-Akt) was described previously (33). An adenovirus carrying green fluorescent protein (Ad-GFP) was used as the internal control (34). Aortic segments were infected with adenovirus (5×10^8 pfu) for 4 h in FBS-free DMEM and then transferred to DMEM with 10% FBS with the addition of 25 mmol/L mannitol (NG), or 25 mmol/L glucose (HG) and/or GW1516 (0.1 μmol/L), for 36 h. Transfection efficiency was verified by monitoring the green fluorescence of Ad-GFP on the endothelium side while also preparing mouse aorta under confocal microscope.

Primary culture of mouse aortic endothelial cells. The method was modified based on the early reported procedures (35). In brief, mice were anesthetized with an intraperitoneal injection of pentobarbital sodium (40 mg/kg). Heparin (100 units/mL in PBS) was infused into the circulation from the left ventricle. The aortae were dissected in DMEM and incubated with collagenase type II for 8 min at 37°C. Detached endothelial cells were collected by centrifugation, resuspended in 20% FBS-DMEM, and then cultured in endothelial cell growth medium supplemented with bovine brain extract (Lonza, Walkersville, MD) until confluency. The cultured endothelial cells were then incubated in NG or HG medium with or without the presence of different drugs

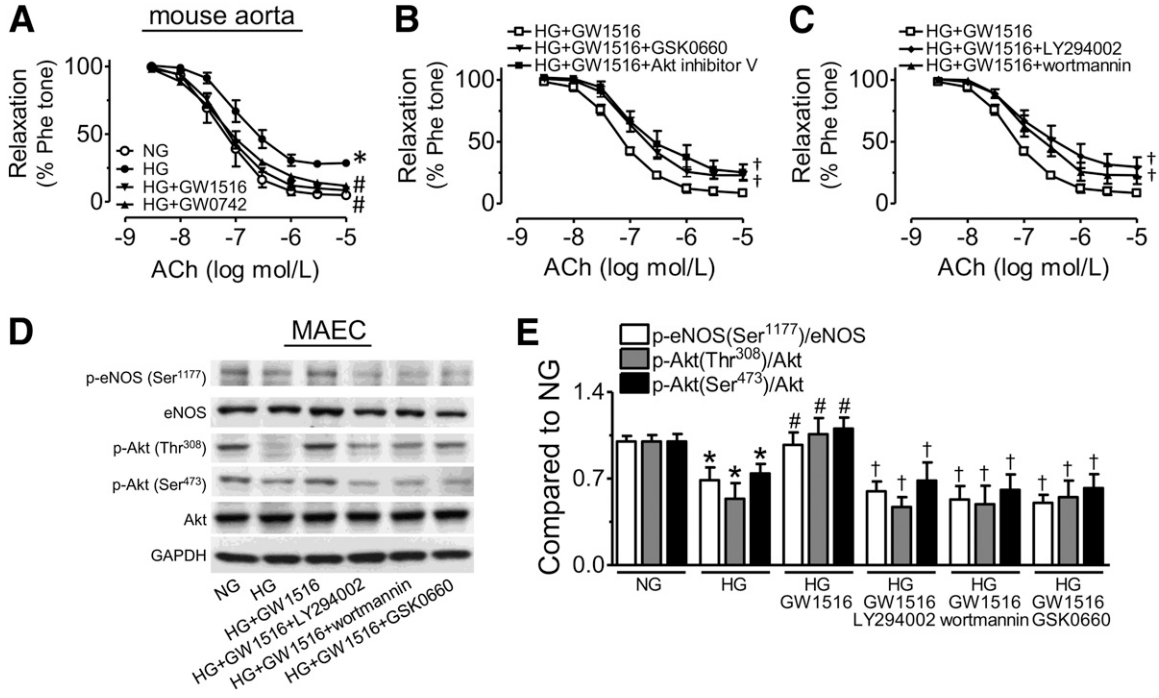

FIG. 1. Effects of PPARδ, PI3K, or Akt inhibitors on EDRs in mouse aortae. *A*: HG impairs EDRs of aortae from C57BL/6J mice, an effect that is reversed by GW0742 or GW1516 (PPARδ agonist, 0.1 μmol/L, 36 h). *B*: The beneficial effect of GW1516 is reversed by GSK0660 (PPARδ antagonist, 1 μmol/L) or Akt inhibitor V (5 μmol/L). *C*: The beneficial effect of GW1516 is reversed by LY294002 (PI3K inhibitor, 5 μmol/L) or wortmannin (PI3K inhibitor, 0.1 μmol/L). *D*: Western blot showing that HG reduces eNOS phosphorylation at Ser^{1177}, and reduces Akt phosphorylation at Thr^{308} and Ser^{473}. These effects are reversed by GW1516 (0.1 μmol/L). The beneficial effects of GW1516 are abrogated by LY294002 (PI3K inhibitor, 5 μmol/L), wortmannin (PI3K inhibitor, 0.1 μmol/L), or GSK0660 (PPARδ antagonist, 1 μmol/L). *E*: Densitometry of Western blots showing the effect of GW1516, and the antagonists of its action on eNOS and Akt phosphorylations in primary MAECs treated with HG (30 mmol/L, 36 h). eNOS, 140 kDa; Akt, 60 kDa. Results are means ± SEM of six mice. *$P < 0.05$ vs. NG; #$P < 0.05$ vs. HG; †$P < 0.05$ vs. HG+GW1516.

for 36 h before the measurement of nitric oxide (NO) using laser confocal fluorescence microscopy.

Transient transfection of mouse aortic endothelial cells. Mouse aortic endothelial cells (MAECs) were transfected with either a constitutively active Akt plasmid (CA-Akt), a dominant-negative Akt construct (DN-Akt), or control plasmid by electroporation using the Nucleofector II machine (Amaxa/Lonza, Walkersville, MD) according to the procedure provided by the manufacturer. DNA plasmids were provided by Dr. Wu Zhenguo (Hong Kong University of Science and Technology, Hong Kong, China) (36). About 70% of endothelial cells were successfully transfected using these protocols, as indicated by control transfection using a GFP-expressing pCAGGS vector.

Measurement of NO production. Fluorimetric measurements were performed on primary MAECs using the Olympus Fluoview FV1000 laser scanning confocal system. 4-Amino-5-methylamino-2',7'-difluorofluorescein diacetate (DAF-FM DA; Molecular Probes, Eugene, OR) was used as the NO indicator. The amount of NO in response to 1 μmol/L A23187 was evaluated by measuring the fluorescence intensity excited at 495 nm and emitted at 515 nm. The cells were stimulated with the calcium ionophore A23187 because there was no calcium or NO signal in response to ACh in the cultured MAECs. Changes in intracellular NO production were displayed as relative fluorescence intensity (F_1/F_0, where F_0 = control and F_1 = after A23187).

Western blotting. Protein samples prepared from mouse aortae or MAEC homogenates were electrophoresed through a 7.5 or 10% SDS-PAGE gel and transferred onto an immobilon-P polyvinylidene difluoride membrane (Millipore Corp., Bedford, MA). Nonspecific binding sites were blocked with 1% BSA in 0.05% Tween-20 TBS. The blots were incubated overnight at 4°C with the primary antibodies anti–phospho-endothelial nitric oxide synthase (eNOS) at Ser^{1177} (1:1,000; Upstate Biotechnology, Lake Placid, NY); anti–phospho-Akt at Ser^{473} and Thr^{308}, anti-Akt1 (1:1,000; Cell Signaling Technology, Danvers, MA), and anti-eNOS (1:1,000; BD Transduction Laboratory, San Diego, CA), followed by horseradish peroxidase–conjugated secondary antibody (DakoCytomation, Carpinteria, CA). Anti-GAPDH (1:5,000; Ambion, Cambridge, U.K.) was used to normalize the protein loading.

Statistics. Results represent means ± SEM from different groups. The protein expression was quantified by densitometer (FluorChem; Alpha Innotech, San Leandro, CA), normalized to GAPDH, and then compared with control. Comparisons among groups were made using ANOVA followed by an unpaired Student *t* test. The *P* values <0.05 were accepted to indicate statistically significant differences.

RESULTS

PI3K/Akt contributes to the beneficial effect of PPARδ agonists on endothelium-dependent vasodilatation impaired by HG. Both PPARδ agonist GW0742 (0.1 μmol/L)

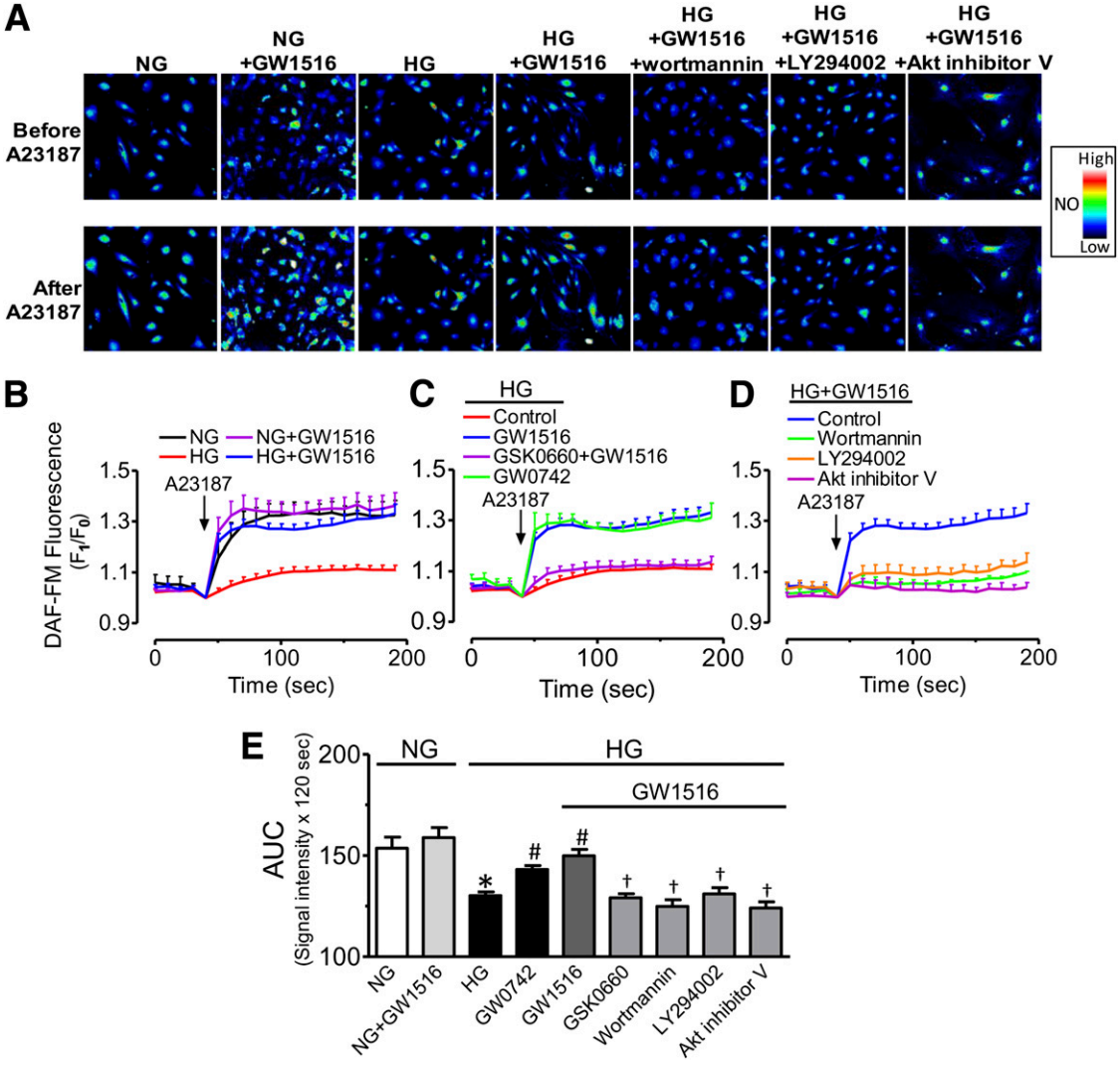

FIG. 2. The effect of GW1516 on NO production in endothelial cells (MAECs). *A*: Representative images of DAF-FM DA fluorescence signal in MAECs in response to Ca^{2+} ionophore A23187 (0.1 μmol/L) under a confocal microscope, analyzed by comparing fluorescence intensity before (F0) and after (F1) the addition of A23187. *B–D*: Summarized results showing the levels of NO production in MAECs treated with GW1516 (0.1 μmol/L) or GW0742 (0.1 μmol/L), in the presence or absence of GSK0660 (1 μmol/L), LY294002 (5 μmol/L), wortmannin (0.1 μmol/L), or Akt inhibitor V (5 μmol/L) in MAECs exposed to NG or HG. *E*: Summarized data using the area under the curve (AUC) starting from the addition of A23187 for 120 s of *B–D*. Results are means ± SEM of six to eight experiments. **P* < 0.05 vs. NG; #*P* < 0.05 vs. HG; †*P* < 0.05 vs. HG+GW1516. Bar, 200 μm. (A high-quality digital representation of this figure is available in the online issue.)

and GW1516 (0.1 μmol/L) augmented EDRs that were impaired by exposure to HG in aortae from C57BL/6J mice (Fig. 1*A*). The effect of GW1516 was abolished by coincubation with PPARδ antagonist GSK0660 (1 μmol/L) (Fig. 1*B*). Coincubation with LY294002 (PI3K inhibitor, 5 μmol/L), wortmannin (PI3K inhibitor, 0.1 μmol/L), or Akt inhibitor V (Akt inhibitor, 5 μmol/L) also diminished the effect of GW1516 to restore EDRs in aortic rings exposed to HG (Fig. 1*B* and *C*). GW1516 or GW0742 did not alter EDR in aortic rings in NG (Supplementary Fig. 1). In HG-treated (30 mmol/L, 36 h) primary MAECs, eNOS phosphorylation at Ser^{1177} and Akt phosphorylation at Ser^{473} and Thr^{308} were decreased. These effects were reversed by GW1516 (0.1 μmol/L). Coincubation with GSK0660, LY294002, or wortmannin inhibited the effect of GW1516 (Fig. 1*D–G*). Specificity of GW1516 was further confirmed in PPARδ WT and KO mice (Supplementary Fig. 2).

PPARδ agonist enhances the NO production in MAECs. In MAECs, the addition of the Ca^{2+} ionophore A23187 (0.1 μmol/L) induced a rise of the DAF-FM DA fluorescence, which reflects the level of NO production in

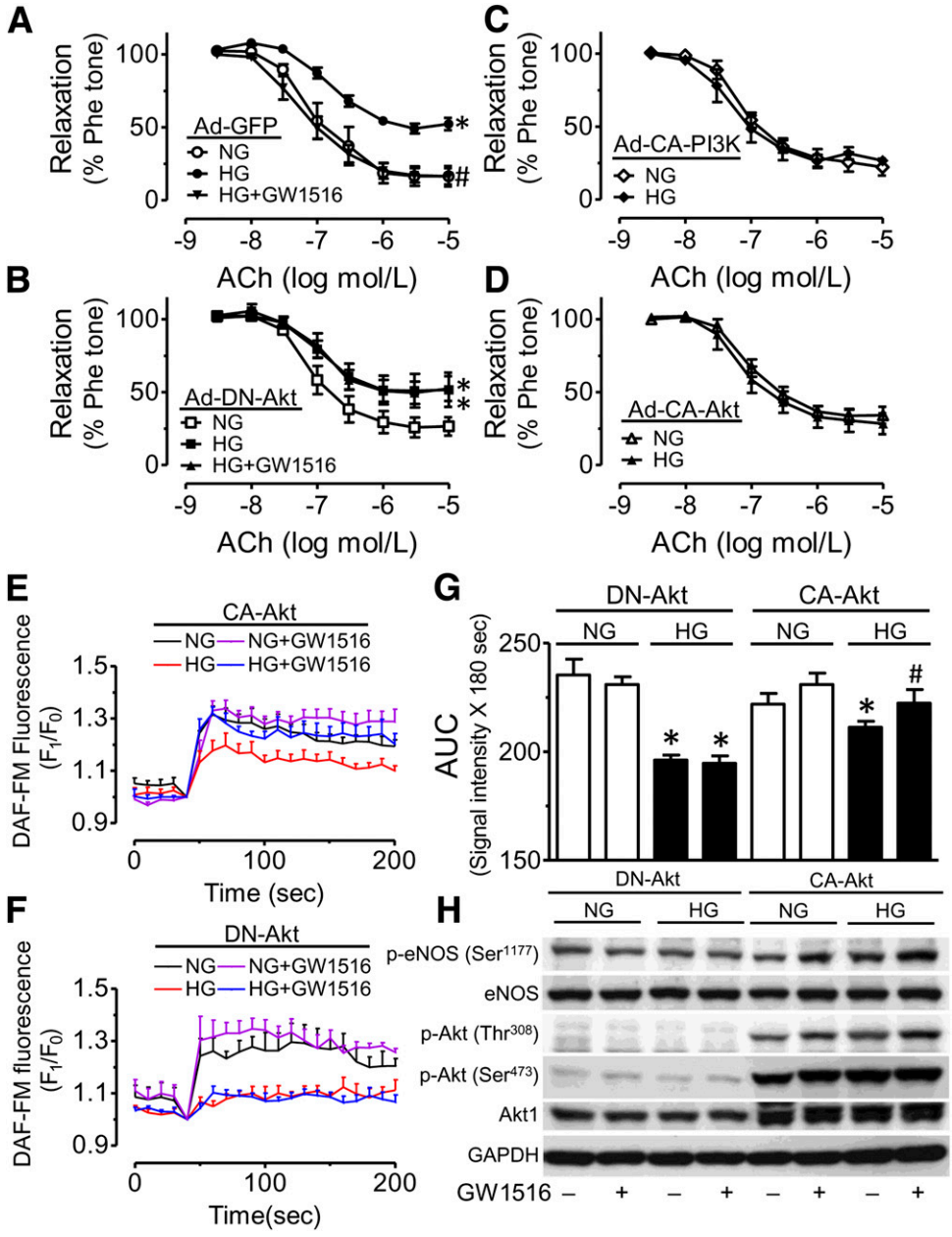

FIG. 3. The effect of Akt activity inhibition on the EDRs in mouse aortae and NO production in MAECs. Effects of Ad-GFP (*A*), Ad-DN-Akt (*B*), Ad-CA-PI3K (*C*), and Ad-CA-Akt (*D*) on EDRs in mouse aortae treated with GW1516 (0.1 μmol/L) and/or HG (30 mmol/L, 36 h). Mouse aortae were exposed to adenovirus for 4 h in serum-free DMEM, and then changed to DMEM with 10% FBS, before vasoreactivity was measured in the myograph. Effects of CA-Akt (*E*) or DN-Akt (*F*) transfection on NO production in MAECs coincubated with GW1516 (0.1 μmol/L) and/or HG (30 mmol/L, 36 h). MAECs were transiently transfected with CA-Akt or DN-Akt plasmid by electroporation. *G*: Summarized data using the area under the curve (AUC) starting from the addition of A23187 for 120 s of *E* and *F*. *H*: Representative Western blot to show the effect of CA-Akt and DN-Akt on Akt and eNOS phosphorylation in MAECs. p-eNOS (Ser^{1177}) and eNOS, 140 kDa; p-Akt (Thr^{308} and Ser^{473}) and Akt, 60 kDa. Experiments were repeated five times using MAECs from different mice. Results are means ± SEM of five to six experiments. *$P < 0.05$ vs. NG from each group; #$P < 0.05$ vs. HG from each group.

the NG group, which was similar in cells treated with GW1516 in the NG group (Fig. 2*A*, *B*, and *E*). HG (30 mmol/L, 36 h) reduced NO production, which was restored by cotreatment with 0.1 μmol/L GW1516 (Fig. 2*A*, *B*, and *E*). GW0742 at 0.1 μmol/L produced a similar effect as GW1516 in HG-treated MAECs, whereas GSK0660 (1 μmol/L) antagonized the effect of GW1516 (0.1 μmol/L) (Fig. 2*A*, *C*, and *E*). Coincubation with LY294002 (5 μmol/L), wortmannin (0.1 μmol/L), or Akt inhibitor V (5 μmol/L) also inhibited the effect of GW1516 (Fig. 2*A*, *D*, and *E*).

Inhibition of Akt activity diminishes the effect of GW1516 on mouse aortae and MAECs. Ad-GFP served as control to verify that adenoviral infection did not affect the EDRs of mouse aortae (Fig. 3*A*). Inhibition of Akt activity by Ad-DN-Akt, the adenovirus expressing dominant-negative Akt, abolished the effect of GW1516 on EDRs in HG-treated aortae from C57BL/6 mice (Fig. 3*B*). Conversely, increasing PI3K or Akt activity by Ad-CA-PI3K or Ad-CA-Akt, the adenoviruses expressing constitutively active PI3K or Akt, reversed HG-impaired EDRs in mouse aortae (Fig. 3*C* and *D*). To further confirm the role of Akt in the effect of GW1516 on NO production in MAECs, we found that CA-Akt slightly increased NO production in HG-treated MAECs (Fig. 3*E* and *G*) without affecting other groups, as compared with data presented in Fig. 2*B*. Suppression of Akt activity by DN-Akt inhibited the restoration of NO production by GW1516 in HG-treated MAECs (Fig. 3*F* and *G*). DN-Akt suppressed, whereas CA-Akt increased, Akt phosphorylation (Fig. 3*H*) at basal level. CA-Akt also increased eNOS phosphorylation stimulated by GW1516 (Fig. 3*H*).

PPARδ agonists improve endothelial function in aortae from *db/db* mice. Treatment with PPARδ agonists GW1516 (0.1 μmol/L, 24 h) or GW0742 (0.1 μmol/L, 24 h) markedly improved EDRs, which were impaired in aortae from *db/db* mice (Fig. 4*A*). Coincubation with GSK0660 (1 μmol/L) antagonized the beneficial effect of GW1516 (0.1 μmol/L) (Fig. 4*A*). Coincubation with LY294002 (5 μmol/L), wortmannin (0.1 μmol/L), or Akt inhibitor V (5 μmol/L) also attenuated the beneficial effect of GW1516 on *db/db* mouse aortae (Fig. 4*B*). To examine the effect of PPARδ activation in vivo, GW1516 was given by oral gavage (5 mg/kg/day, 7 days) to *db/db* mice. EDRs in aortae from *db/db* mice were significantly reduced as compared with those from *db/m*$^+$ mice. The impaired EDRs were improved after GW1516 treatment (Fig. 4*C*). By contrast, endothelium-independent relaxations to SNP were similar in *db/m*$^+$, *db/db*, and *db/db* treated with GW1516 (Fig. 4*D*).

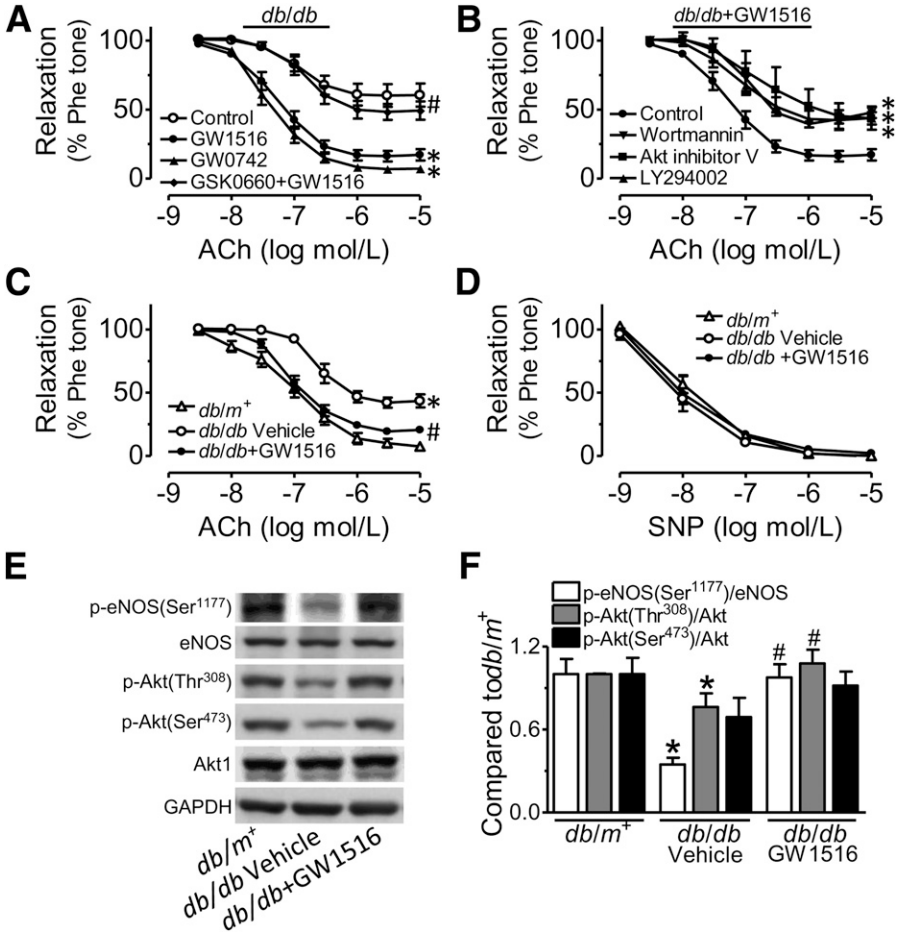

FIG. 4. The effect of GW1516 treatment on endothelial function in *db/db* mice. *A*: PPARδ agonist GW0742 (0.1 μmol/L, 24 h) or GW1516 (0.1 μmol/L, 24 h) improved EDRs in aortae from *db/db* mice. The beneficial effect of GW1516 was abrogated by coincubation with GSK0660 (PPARδ antagonist, 1 μmol/L). *B*: The beneficial effect of GW1516 in aortae from *db/db* mice is abrogated by LY294002 (5 μmol/L), wortmannin (0.1 μmol/L), or Akt inhibitor V (5 μmol/L). *C*: GW1516 treatment (5 mg/kg/day, 7–10 days) improved EDRs in aortae from *db/db* mice, without affecting endothelium-independent relaxations to SNP (*D*). *E* and *F*: GW1516 treatment increased phosphorylations of eNOS and Akt in *db/db* mouse aortae. Results are means ± SEM of *n* mice (*n* specified in Supplementary Table 1). **P* < 0.05 vs. *db/m*$^+$; #*P* < 0.05 vs. *db/db*.

Phosphorylations of eNOS at Ser^{1177} and of Akt at Thr^{308} were restored in aortae from GW1516-treated *db/db* mice (Fig. 4*E* and *F*).

GW1516 treatment improves FMD and insulin-induced vasodilatation in arteries from DIO mice. FMD was measured in mesenteric resistance arteries of normal or DIO C57BL/6 mice and of *db/db* mice. FMD was induced by a pressure change of 20 mmHg, which equals an initial shear stress of ~15 dynes/cm^2 in pressurized arteries. FMD was improved in mesenteric resistance arteries from DIO mice or *db/db* mice treated with GW1516 (Fig. 5*A–C*). GW1516 treatment also enhanced insulin-induced vasodilatation in arteries from DIO mice (Fig. 5*B*). ACh-induced relaxation in aortae or FMD in resistance arteries was unaffected in control mice treated with GW1516 (Fig. 5*C* and Supplementary Fig. 1).

GW1516 treatment in vivo improves endothelial function in DIO mice in a PPARδ-specific manner. *PPARδ* KO and *PPARδ* WT mice were fed with a high-fat diet for 12 weeks. GW1516 was administered by oral gavage (5 mg/kg/day, 7 days). EDRs were impaired in aortae from DIO *PPARδ* KO or DIO *PPARδ* WT mice compared with control mice of the same genotype on a normal diet (Fig. 6*A* and *B*). GW1516 treatment in vivo restored EDRs in aortae from DIO *PPARδ* WT mice (Fig. 6*A*), but not in those from DIO *PPARδ* KO mice (Fig. 6*B*). Again, endothelium-independent relaxations to SNP were similar in all groups (Fig. 6*C* and *D*). Reduced eNOS and Akt phosphorylation upon high-fat feeding in DIO mice was restored after GW1516 treatment only in aortae from *PPARδ* WT mice, not in those from *PPARδ* KO mice (Fig. 6*E* and *F*).

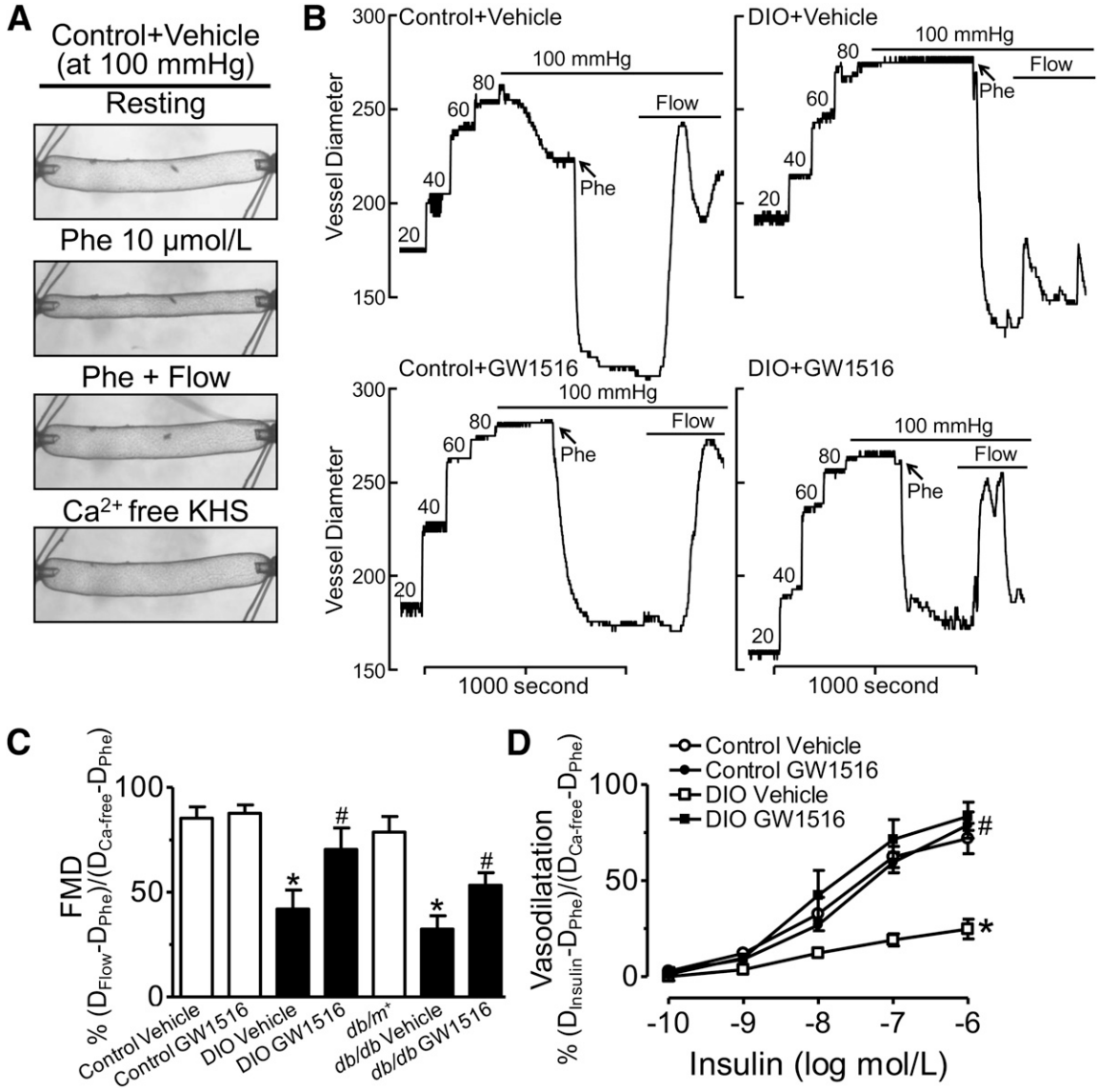

FIG. 5. GW1516 treatment improves FMD and insulin-induced vasodilatation in pressurized mesenteric arteries of diet-induced obese mice. GW1516 was administered by oral gavage (5 mg/kg/day, 7–10 days) to DIO C57BL/6 and *db/db* mice. *A*: Representative image of mesenteric resistance arteries from control C57BL/6 mice pressurized at 100 mmHg. *B*: Representative trace of FMD from each group. Pressure rise was induced in stepwise order (20–100 mmHg). Phe (10 μmol/L) was added after arteries stabilized at 100 mmHg to induce contraction before FMD was examined. *C*: Summarized FMD response in arteries from all the groups. *D*: Summarized data of insulin-induced vasodilatation in mesenteric resistance arteries from C57BL/6 control and DIO mice. Results are means ± SEM of four to five mice. *$P < 0.05$ vs. control or *db/m*$^+$; #$P < 0.05$ vs. vehicle.

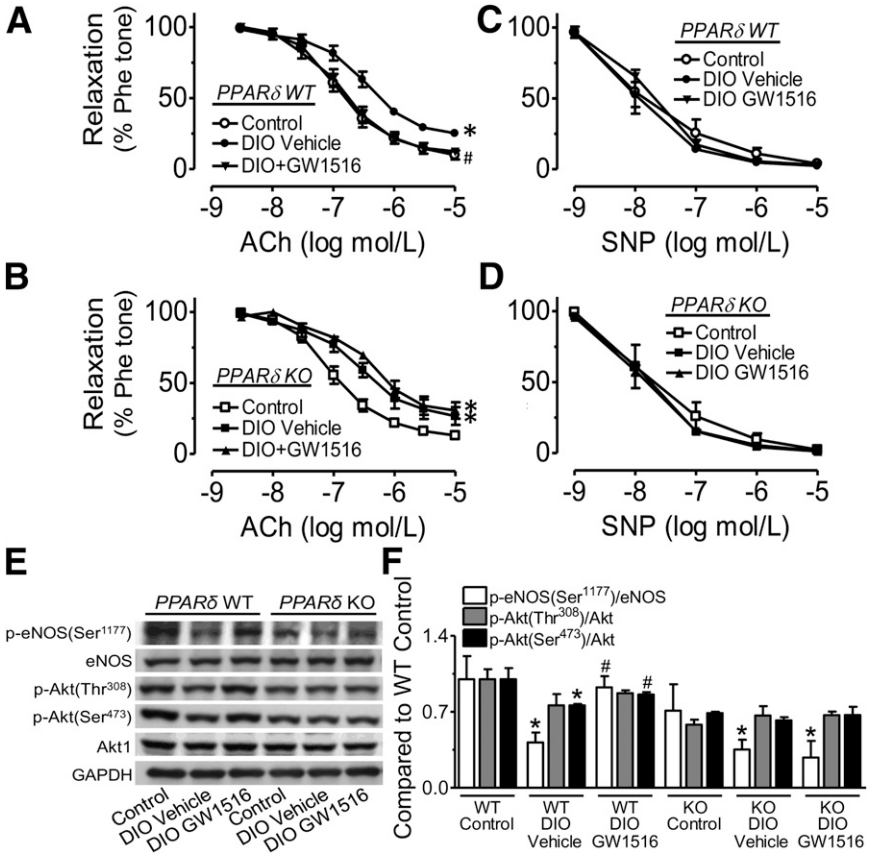

FIG. 6. GW1516 treatment in vivo improved endothelial function in aortae from *PPARδ* WT mice but not in *PPARδ* KO mice after high-fat diet (DIO). GW1516 was administered by oral gavage (5 mg/kg/day, 7–10 days) to DIO *PPARδ* WT and age-matched *PPARδ* KO fed on high-fat diet for 3 months. Effects of GW1516 treatment on EDRs in aortae from *PPARδ* WT (*A*) and *PPARδ* KO (*B*) after high-fat diet–induced obesity compared with control mice on normal diet. Endothelium-independent relaxations to SNP in aortae from *PPARδ* WT (*C*) and *PPARδ* KO (*D*). *E* and *F*: Phosphorylation of eNOS and Akt in aortae from DIO *PPARδ* WT mice increased after GW1516 treatment, an effect that was not observed in those from DIO *PPARδ* KO mice. Results are means ± SEM of *n* mice (*n* specified in Supplementary Table 1). **P* < 0.05 vs. control (normal diet) from each group; #*P* < 0.05 vs. DIO from each genotype.

DISCUSSION

We demonstrated that PPARδ activation improved endothelial function in diabetic mice through the activation of PI3K/Akt. PPARδ agonists GW1516 and GW0742 improve EDRs in aortae that were impaired by a 36-h exposure to HG.

First, the effects of PPARδ ligands were PPARδ specific, which was verified by using three approaches: *1*) two selective PPARδ agonists, GW1516 and GW0742, exhibited similar effects in improving EDRs in aortae and in augmenting the NO production in MAECs; *2*) the selective PPARδ antagonist GSK0660 blocked the beneficial effect of GW1516; and *3*) the beneficial effect of GW1516 was absent in arteries from *PPARδ* KO mice. Second, the effect of PPARδ activation in mouse aortae and in MAECs is mediated through PI3K/Akt signaling based on the following observations: *1*) the effect of PPARδ agonists to improve NO production in arteries was reversed by pharmacological inhibitors of both PI3K and Akt; *2*) the PPARδ agonist–stimulated phosphorylation of Akt and eNOS and the PPARδ-mediated NO production in MAECs were also sensitive to PI3K/Akt inhibition; *3*) the suppression of Akt activity by DN-Akt diminished the effect of GW1516 to restore impaired EDRs in mouse aortae and attenuated the effect of GW1516 to enhance NO production as well as phosphorylation of eNOS and Akt in MAECs exposed to HG; and *4*) adenoviral constructs encoding the constitutively active Akt or PI3K restored the impaired EDRs in mouse aortae and augmented NO production in MAECs exposed to HG. Finally, we documented the beneficial effects of PPARδ activation on endothelial function by showing that oral GW1516 treatment improves EDRs and FMDs in arteries from *db/db* and DIO *PPARδ* WT but not KO mice.

Although PPARδ is expressed in vascular cells (3,18), the role of PPARδ in the regulation of cardiovascular function has not been fully characterized. It is known that PPARδ activation induces angiogenesis and vasculogenesis (19,21). In mouse models of atherosclerosis, PPARδ activation decreases the size of atherosclerotic lesions and suppresses the expression of endothelial adhesion molecules (24,26,37). However, there is no study examining the impact of PPARδ agonists on diabetic vasomotor dysfunction. The current study provides novel evidence demonstrating that PPARδ agonists can restore endothelium-dependent dilatory function in isolated aortae from *db/db* mice and in aortae subjected to HG challenge. This notion is supported by the beneficial effect of GW1516 treatment in vivo in both diabetic and obese mice. Given that PPARδ agonists can ameliorate dyslipidemia, the beneficial effect of GW1516 might be partially due to its favorable modulation of lipid metabolism in vivo and its protective effect against lipid-induced endothelial dysfunction (Supplementary Table 1 and Fig. 3). However, in

the current study, glucose metabolism was not significantly affected by in vivo GW1516 treatment in *db/db* mice and in DIO *PPARδ* WT and KO mice, although the triglyceride level decreased after GW1516 treatment, which might also contribute to the beneficial effect on vascular function (Supplementary Table 1). Furthermore, a beneficial effect of PPARδ agonists was observed using ex vivo organ culture of isolated mouse aortic segment, as well as cultured endothelial cells, where ambient lipid and glucose levels were constant. In addition, unlike the previous study, which showed that GW1516 decreased GLUT1 activation and expression (38), in the current study, GLUT1 activation and expression were not altered in the endothelial cells by GW1516 (Supplementary Fig. 4). The results from these experiments strongly suggest that PPARδ agonists have a direct effect on endothelium-dependent vasodilatation independent of any effects on lipid or glucose metabolism.

Existing evidence indicates that PPARs benefit endothelial function. Although the function of PPARδ is less studied, PPARγ agonists pioglitazone and rosiglitazone improve EDR in resistance arteries and reduce the angiotensin II–induced hypertension in rats (39). PPARα and PPARγ agonists inhibit the thrombin-activated endothelin-1 synthesis in vitro (40). PPARγ also elevates NO bioavailability by increasing its synthesis (41), through activation of p38 MAPK (42), and/or by decreasing its degradation by superoxide anions (43). PPAR agonists also improve vascular function in diabetic patients (44,45). Both animal and clinical studies suggest that PPARs can be potential targets for pharmaceutical intervention in the protection of endothelial function in diabetes. Given the recently reported adverse effect of rosiglitazone on cardiovascular outcomes in diabetic patients (46,47), PPARδ could be an alternative target for the treatment of atherosclerosis, hypertension, and other cardiovascular events in diabetic patients.

The current study shows that the activation of the PI3K/Akt pathway is essential for the beneficial effect of PPARδ agonists on endothelial function. The PPARδ agonist promotes cell survival through PI3K/Akt-dependent mechanisms (48). The interaction between PPARδ and PI3K/Akt was also found in other cell type (49). A recent study described that GW1516 promotes vasculogenesis through genomic transcription and nongenomic activation of PI3K/Akt via interaction with p85α, a regulatory subunit of PI3K (21). In addition, GW0742 and L-165041 at higher concentrations (>1 μmol/L) can directly induce vasodilatation, NO generation, and eNOS phosphorylation, which are partially related to activation of the PI3K/Akt pathway in the rat aorta (27). The present data supported the aforementioned observations that PI3K/Akt is one of the most likely downstream mechanisms for the vascular-protective effects of PPARδ activation. Furthermore, we have provided evidence that the benefit of PPARδ on vasodilation requires the activation of PI3K/Akt. In addition, GW1516 did not alter p38, ERK, endothelin-1 activity, or caspase activity in aortae or endothelial cells (Supplementary Figs. 5–8).

Recently, a beneficial effect of GW1516 on dyslipidemia in humans has been observed (13,14). However, the cardiovascular safety and outcome of PPARδ ligands is still under investigation. The current study indicates that PPARδ activation is likely to reduce the risk of adverse cardiovascular events, as it improves the vasodilator function of the endothelium exposed to HG conditions in vitro or ex vivo. These novel findings may help to enhance the prospective of the use of safe PPARδ ligands in combating vascular dysfunction in diabetes and obesity.

ACKNOWLEDGMENTS

This work was supported by grants from the Natural Science Foundation of China/Research Grants Council of Hong Kong Joint Research Scheme (N_CUHK428/09), the National Science Foundation of China (30890041 and 30931160434), the Ministry of Science and Technology of China (973 programs 2010CB912502 and 2012CB517805), and the Hong Kong General Research Fund (2140676 and 465611).

No potential conflicts of interest relevant to this article were reported.

X.Y.T. and W.T.W. designed and conducted the experiments, analyzed the data, and prepared the manuscript. N.W. and Y.H. designed the experiments and prepared the manuscript. Y. Lu, W.S.C., J.L., L.L., and Y.Li. conducted the experiments. S.S.-T.L. provided the transgenic mice. Z.Y.C., J.P.C., and X.Y. assisted with discussion and reviewed the manuscript. Y.H. is the guarantor of this work and, as such, had full access to all the data in the study and takes responsibility for the integrity of the data and the accuracy of the data analysis.

The authors thank Dr. Wu Zhenguo (Hong Kong University of Science and Technology) for providing the DNA plasmid and Dr. John J. Shyy (University of California, Riverside, CA) for providing the Ad-DN-Akt adenovirus.

REFERENCES

1. Peters JM, Lee SS, Li W, et al. Growth, adipose, brain, and skin alterations resulting from targeted disruption of the mouse peroxisome proliferator-activated receptor beta(delta). Mol Cell Biol 2000;20:5119–5128
2. Barak Y, Liao D, He W, et al. Effects of peroxisome proliferator-activated receptor delta on placentation, adiposity, and colorectal cancer. Proc Natl Acad Sci USA 2002;99:303–308
3. Tanaka T, Yamamoto J, Iwasaki S, et al. Activation of peroxisome proliferator-activated receptor delta induces fatty acid beta-oxidation in skeletal muscle and attenuates metabolic syndrome. Proc Natl Acad Sci USA 2003;100:15924–15929
4. Wang YX, Lee CH, Tiep S, et al. Peroxisome-proliferator-activated receptor delta activates fat metabolism to prevent obesity. Cell 2003;113:159–170
5. Oliver WR Jr, Shenk JL, Snaith MR, et al. A selective peroxisome proliferator-activated receptor delta agonist promotes reverse cholesterol transport. Proc Natl Acad Sci USA 2001;98:5306–5311
6. Leibowitz MD, Fiévet C, Hennuyer N, et al. Activation of PPARdelta alters lipid metabolism in db/db mice. FEBS Lett 2000;473:333–336
7. Cohen G, Riahi Y, Shamni O, et al. Role of lipid peroxidation and PPAR-δ in amplifying glucose-stimulated insulin secretion. Diabetes 2011;60:2830–2842
8. Serrano-Marco L, Rodríguez-Calvo R, El Kochairi I, et al. Activation of peroxisome proliferator-activated receptor-β/-δ (PPAR-β/-δ) ameliorates insulin signaling and reduces SOCS3 levels by inhibiting STAT3 in interleukin-6-stimulated adipocytes. Diabetes 2011;60:1990–1999
9. Kang K, Reilly SM, Karabacak V, et al. Adipocyte-derived Th2 cytokines and myeloid PPARdelta regulate macrophage polarization and insulin sensitivity. Cell Metab 2008;7:485–495
10. Lee CH, Olson P, Hevener A, et al. PPARdelta regulates glucose metabolism and insulin sensitivity. Proc Natl Acad Sci USA 2006;103:3444–3449
11. Qin X, Xie X, Fan Y, et al. Peroxisome proliferator-activated receptor-delta induces insulin-induced gene-1 and suppresses hepatic lipogenesis in obese diabetic mice. Hepatology 2008;48:432–441
12. Matsushita Y, Ogawa D, Wada J, et al. Activation of peroxisome proliferator-activated receptor delta inhibits streptozotocin-induced diabetic nephropathy through anti-inflammatory mechanisms in mice. Diabetes 2011;60:960–968
13. Sprecher DL, Massien C, Pearce G, et al. Triglyceride:high-density lipoprotein cholesterol effects in healthy subjects administered a peroxisome proliferator activated receptor delta agonist. Arterioscler Thromb Vasc Biol 2007;27:359–365
14. Risérus U, Sprecher D, Johnson T, et al. Activation of peroxisome proliferator-activated receptor (PPAR)delta promotes reversal of multiple metabolic abnormalities, reduces oxidative stress, and increases fatty acid oxidation in moderately obese men. Diabetes 2008;57:332–339

15. Burkart EM, Sambandam N, Han X, et al. Nuclear receptors PPARbeta/delta and PPARalpha direct distinct metabolic regulatory programs in the mouse heart. J Clin Invest 2007;117:3930–3939
16. Cheng L, Ding G, Qin Q, et al. Cardiomyocyte-restricted peroxisome proliferator-activated receptor-delta deletion perturbs myocardial fatty acid oxidation and leads to cardiomyopathy. Nat Med 2004;10:1245–1250
17. Georgiadi A, Lichtenstein L, Degenhardt T, et al. Induction of cardiac Angptl4 by dietary fatty acids is mediated by peroxisome proliferator-activated receptor beta/delta and protects against fatty acid-induced oxidative stress. Circ Res 2010;106:1712–1721
18. Piqueras L, Reynolds AR, Hodivala-Dilke KM, et al. Activation of PPARbeta/delta induces endothelial cell proliferation and angiogenesis. Arterioscler Thromb Vasc Biol 2007;27:63–69
19. He T, Lu T, d'Uscio LV, Lam CF, Lee HC, Katusic ZS. Angiogenic function of prostacyclin biosynthesis in human endothelial progenitor cells. Circ Res 2008;103:80–88
20. He T, Smith LA, Lu T, Joyner MJ, Katusic ZS. Activation of peroxisome proliferator-activated receptor-delta enhances regenerative capacity of human endothelial progenitor cells by stimulating biosynthesis of tetrahydrobiopterin. Hypertension 2011;58:287–294
21. Han JK, Lee HS, Yang HM, et al. Peroxisome proliferator-activated receptor-delta agonist enhances vasculogenesis by regulating endothelial progenitor cells through genomic and nongenomic activations of the phosphatidylinositol 3-kinase/Akt pathway. Circulation 2008;118:1021–1033
22. Liou JY, Lee S, Ghelani D, Matijevic-Aleksic N, Wu KK. Protection of endothelial survival by peroxisome proliferator-activated receptor-delta mediated 14-3-3 upregulation. Arterioscler Thromb Vasc Biol 2006;26:1481–1487
23. Yin KJ, Deng Z, Hamblin M, Zhang J, Chen YE. Vascular PPARδ protects against stroke-induced brain injury. Arterioscler Thromb Vasc Biol 2011;31:574–581
24. Fan Y, Wang Y, Tang Z, et al. Suppression of pro-inflammatory adhesion molecules by PPAR-delta in human vascular endothelial cells. Arterioscler Thromb Vasc Biol 2008;28:315–321
25. Graham TL, Mookherjee C, Suckling KE, Palmer CN, Patel L. The PPARdelta agonist GW0742X reduces atherosclerosis in LDLR(-/-) mice. Atherosclerosis 2005;181:29–37
26. Li AC, Binder CJ, Gutierrez A, et al. Differential inhibition of macrophage foam-cell formation and atherosclerosis in mice by PPARalpha, beta/delta, and gamma. J Clin Invest 2004;114:1564–1576
27. Jiménez R, Sánchez M, Zarzuelo MJ, et al. Endothelium-dependent vasodilator effects of peroxisome proliferator-activated receptor beta agonists via the phosphatidyl-inositol-3 kinase-Akt pathway. J Pharmacol Exp Ther 2010;332:554–561
28. Zarzuelo MJ, Jiménez R, Galindo P, et al. Antihypertensive effects of peroxisome proliferator-activated receptor-β activation in spontaneously hypertensive rats. Hypertension 2011;58:733–743
29. Müller-Brüsselbach S, Kömhoff M, Rieck M, et al. Deregulation of tumor angiogenesis and blockade of tumor growth in PPARbeta-deficient mice. EMBO J 2007;26:3686–3698
30. Chan YC, Leung FP, Wong WT, et al. Therapeutically relevant concentrations of raloxifene dilate pressurized rat resistance arteries via calcium-dependent endothelial nitric oxide synthase activation. Arterioscler Thromb Vasc Biol 2010;30:992–999
31. Wong WT, Tian XY, Chen Y, et al. Bone morphogenic protein-4 impairs endothelial function through oxidative stress-dependent cyclooxygenase-2 upregulation: implications on hypertension. Circ Res 2010;107:984–991
32. Tang Z, Wang Y, Fan Y, Zhu Y, Chien S, Wang N. Suppression of c-Cbl tyrosine phosphorylation inhibits neointimal formation in balloon-injured rat arteries. Circulation 2008;118:764–772
33. Chen Z, Peng IC, Sun W, et al. AMP-activated protein kinase functionally phosphorylates endothelial nitric oxide synthase Ser633. Circ Res 2009;104:496–505
34. Wang N, Verna L, Chen NG, et al. Constitutive activation of peroxisome proliferator-activated receptor-gamma suppresses pro-inflammatory adhesion molecules in human vascular endothelial cells. J Biol Chem 2002;277:34176–34181
35. Kobayashi M, Inoue K, Warabi E, Minami T, Kodama T. A simple method of isolating mouse aortic endothelial cells. J Atheroscler Thromb 2005;12:138–142
36. Xu Q, Wu Z. The insulin-like growth factor-phosphatidylinositol 3-kinase-Akt signaling pathway regulates myogenin expression in normal myogenic cells but not in rhabdomyosarcoma-derived RD cells. J Biol Chem 2000;275:36750–36757
37. Takata Y, Liu J, Yin F, et al. PPARdelta-mediated antiinflammatory mechanisms inhibit angiotensin II-accelerated atherosclerosis. Proc Natl Acad Sci USA 2008;105:4277–4282
38. Riahi Y, Sin-Malia Y, Cohen G, et al. The natural protective mechanism against hyperglycemia in vascular endothelial cells: roles of the lipid peroxidation product 4-hydroxydodecadienal and peroxisome proliferator-activated receptor delta. Diabetes 2010;59:808–818
39. Diep QN, El Mabrouk M, Cohn JS, et al. Structure, endothelial function, cell growth, and inflammation in blood vessels of angiotensin II-infused rats: role of peroxisome proliferator-activated receptor-gamma. Circulation 2002;105:2296–2302
40. Delerive P, Martin-Nizard F, Chinetti G, et al. Peroxisome proliferator-activated receptor activators inhibit thrombin-induced endothelin-1 production in human vascular endothelial cells by inhibiting the activator protein-1 signaling pathway. Circ Res 1999;85:394–402
41. Kleinhenz JM, Kleinhenz DJ, You S, et al. Disruption of endothelial peroxisome proliferator-activated receptor-gamma reduces vascular nitric oxide production. Am J Physiol Heart Circ Physiol 2009;297:H1647–H1654
42. Ptasinska A, Wang S, Zhang J, Wesley RA, Danner RL. Nitric oxide activation of peroxisome proliferator-activated receptor gamma through a p38 MAPK signaling pathway. FASEB J 2007;21:950–961
43. Hwang J, Kleinhenz DJ, Lassègue B, Griendling KK, Dikalov S, Hart CM. Peroxisome proliferator-activated receptor-gamma ligands regulate endothelial membrane superoxide production. Am J Physiol Cell Physiol 2005;288:C899–C905
44. Campia U, Matuskey LA, Panza JA. Peroxisome proliferator-activated receptor-gamma activation with pioglitazone improves endothelium-dependent dilation in nondiabetic patients with major cardiovascular risk factors. Circulation 2006;113:867–875
45. McMahon GT, Plutzky J, Daher E, Bhattacharyya T, Grunberger G, DiCarli MF. Effect of a peroxisome proliferator-activated receptor-gamma agonist on myocardial blood flow in type 2 diabetes. Diabetes Care 2005;28:1145–1150
46. Nissen SE, Wolski K. Effect of rosiglitazone on the risk of myocardial infarction and death from cardiovascular causes. N Engl J Med 2007;356:2457–2471
47. Home PD, Pocock SJ, Beck-Nielsen H, et al.; RECORD Study Group. Rosiglitazone evaluated for cardiovascular outcomes—an interim analysis. N Engl J Med 2007;357:28–38
48. Di-Poï N, Tan NS, Michalik L, Wahli W, Desvergne B. Antiapoptotic role of PPARbeta in keratinocytes via transcriptional control of the Akt1 signaling pathway. Mol Cell 2002;10:721–733
49. Zhang J, Fu M, Zhu X, et al. Peroxisome proliferator-activated receptor delta is up-regulated during vascular lesion formation and promotes post-confluent cell proliferation in vascular smooth muscle cells. J Biol Chem 2002;277:11505–11512